

NUMERICAL PREDICTION OF HOT WATER FLOW AND TEMPERATURE DISTRIBUTION IN THERMAL STORAGE TANK

S.Iwamoto, N.Takayama, M.Imano and N.Nakahara
Kanagawa University
Yokohama 221-8686 Japan
iwamotos@cc.kanagawa-u.ac.jp

ABSTRACT

In order to evaluate energy efficiency of solar hot water systems, a calculation method was developed in this paper that models the unsteady flow and temperature distribution in heat storage tank utilizing Computational Fluid Dynamics (CFD). Compared to actual measurements, adequate calculated results were obtained that agree during both heat storage and supplying hot water. These calculation results can not be easily replicated in actual measurements. Applying these results to a block model that reduces the time required for calculation will be the subject of future study.

INTRODUCTION

To promote further propagation and utilization of hot water supply system based on solar heat, it is necessary to adequately evaluate as to what extent the individual system provides energy-saving effect. The methods of evaluation include experiment, measurement and numerical prediction. Valuable data can be obtained through experiment and measurement, while much labor, time and cost are required because experiment and measurement must be carried out for long period, and this is not easily accomplished. In the numerical prediction, there is a problem of accuracy, but labor, time and cost can be extensively reduced, and the setting condition can be relatively easily adjusted.

A solar heat type hot water supply system comprises heat collector, heat exchanger, heat storage tank, auxiliary heat source, etc. In the numerical prediction, the entire system including various elements and control must be taken into account. In particular, in the numerical prediction for heat storage tank equipped with heat exchanger (hereinafter referred as "heat storage tank") as commonly used in houses, block model is often used. In the block model, the space inside the tank is divided into several blocks in vertical direction and temperature distribution is determined from thermal balance in each block. Because the time required for calculation is relatively short, annual numerical prediction can be easily performed, whereas the accuracy of calculation is not always on satisfactory level.

In the present study, with the purpose of improving the accuracy of numerical prediction, a calculation model was prepared instead of the block model, and this calculation model was used for analysis of unsteady flow and temperature in the heat storage tank by computational fluid dynamics (CFD). Through comparison of the measured results with the calculated results, the accuracy of calculation was confirmed.

OUTLINE OF MEASUREMENT

Measuring system

The measurement data used in the present study was obtained in the performance test of solar heat type hot water supply system, which was carried out in Hamamatsu, Shizuoka Prefecture, Japan, for a period of 51 days from October 28 to December 18, 1997. The measuring system comprised, as shown in Figure 1, solar heat collector, brine pump, heat storage tank, etc. The items of measurement included brine outlet temperature A and brine inlet temperature B, water feeding temperature C, hot water feeding temperature D, hot water supply temperature E, hot water supply system ambient temperature, meteorological data such as wind velocity, quantity of solar radiation, on/off control information of brine pump, power consumption, etc. The values C to E were measured at 2-second time interval, and the other data were determined at one-minute time interval. During the experiment, the brine pump was placed under proper on/off control.

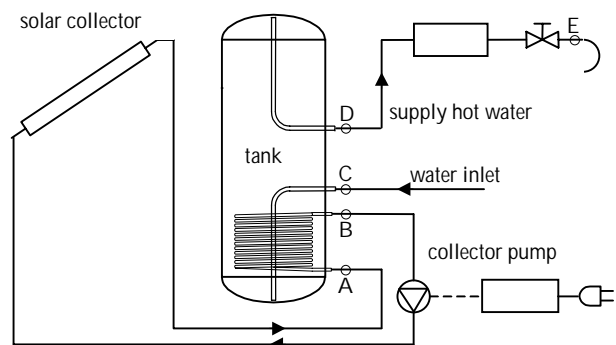


Figure 1. Summary of measurement

Heat storage tank

The heat storage tank used in the measurement had a capacity of about 300 liters and its upper and lower portions were designed each in shape of regular semi-ellipsoid. The heat storage tank was made of chromium steel and was covered with glass wool heat insulation of 50 mm in thickness. The heat exchanger was designed with chromium steel pipes, and it was installed in spiral form with diameter of 400 mm as shown in Figure 1.

Use of measurement data in the calculation

From the measurement data, November 9 was selected as the representative day because brine pump was operated for relatively long time on this day. On/off control information of brine pump and temperature values at A and C were used for calculation, and the measured temperature values at B and D were compared with the calculated results. Figure 2 summarizes heat collection schedule and hot water supply schedule on November 9.

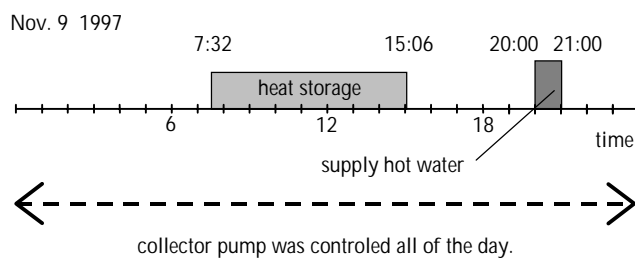


Figure 2. Schedule of measurement

The measurement was performed as the performance test of the solar heat type hot water supply system, and it was not performed with the purpose of comparing the measured values with the calculation results obtained by CFD. Water flow distribution and temperature distribution within the tank were not determined. Detailed comparison cannot be achieved, but by comparing inlet temperature of brine and hot water feeding temperature, the results of the comparison can be used for confirmation and evaluation of calculation accuracy from the viewpoint of thermal balance in the entire tank.

CALCULATION METHOD

Object of calculation

Based on the heat storage tank used in the measurement, the object to be calculated was defined as a space of 265 mm (radius) x 1487 mm (height) as shown in Figure 3. It was assumed that inner space of the heat storage tank was axially symmetric, and analysis was made by regarding the cross-section of

the tank as a 2-dimensional cylindrical coordinate system. Number of division cells was 22 x 120, and deformed cells in an area of 12.5 mm - 16.275 mm were used as the area of calculation. Cross-section of heat exchanger pipe was considered as a square with each side being 12.5 mm in length. The calculation method can be roughly divided to CFD calculation of heat convection inside the tank and calculation of heat transfer from heat exchanger. The details will be described below.

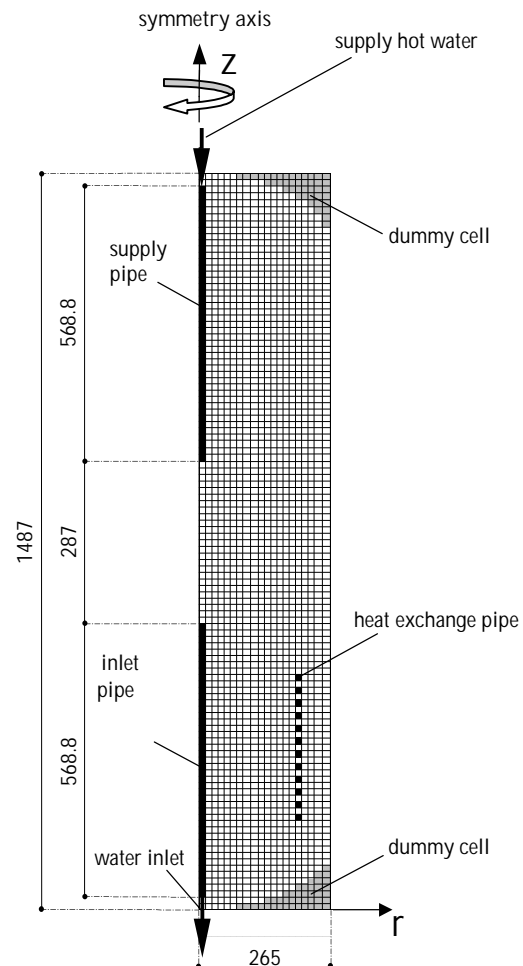


Figure 3. Calculation domain

CFD for heat convection in the tank

To ensure stability in calculation, Viollet type $k-\epsilon$ 2 equation turbulence model was used, and this was applied to 2-dimensional axially symmetric non-isothermal flow. Basic equations are the equations (1) - (7) as shown in Table 1. SIMPLE method was used as solution. In the differential scheme of convective term for each variable, velocity components u and w and water temperature θ were included in QUICK scheme, and k and ϵ in upwind scheme. Time term was included in backward scheme, and all others were treated in central differential scheme. In boundary condition, axis of

symmetry was set as the condition of symmetry. In wall surface boundary condition, log law was used for velocity components. Water temperature was treated in laminar flow condition on outer periphery of heat exchanger pipe and in perfect adiabatic condition on inner wall of the heat storage tank.

Table 1. List of basic equations

$$(1) \frac{\partial}{\partial r}(ru) + \frac{\partial}{\partial z}(rw) = 0$$

$$(2) \frac{\partial}{\partial t}(ru) + \frac{\partial}{\partial r}(ru^2) + \frac{\partial}{\partial z}(ruw) = -r \frac{\partial \pi}{\partial r} + \frac{\partial}{\partial r} \left\{ 2r v_\theta \frac{\partial u}{\partial r} \right\} + \frac{\partial}{\partial z} \left\{ r v_\theta \left(\frac{\partial w}{\partial r} + \frac{\partial u}{\partial z} \right) \right\} - 2v_\theta \frac{u}{r}$$

$$(3) \frac{\partial}{\partial t}(rw) + \frac{\partial}{\partial r}(ruw) + \frac{\partial}{\partial z}(ruw) = -r \frac{\partial \pi}{\partial z} + \frac{\partial}{\partial r} \left\{ r v_\theta \left(\frac{\partial w}{\partial r} + \frac{\partial u}{\partial z} \right) \right\} + \frac{\partial}{\partial z} \left\{ 2r v_\theta \frac{\partial w}{\partial z} \right\} + rg\beta(\theta - \theta_1)$$

$$(4) \frac{\partial}{\partial t}(rk) + \frac{\partial}{\partial r}(ruk) + \frac{\partial}{\partial z}(rkw) = \frac{\partial}{\partial r} \left\{ r v_\theta \frac{\partial k}{\partial r} \right\} + \frac{\partial}{\partial z} \left\{ r v_\theta \frac{\partial k}{\partial z} \right\} + r \left(S - \varepsilon - g\beta \frac{v_\theta}{\sigma_\theta} \frac{\partial \theta}{\partial z} \right)$$

$$(5) \frac{\partial}{\partial t}(r\varepsilon) + \frac{\partial}{\partial r}(r\varepsilon u) + \frac{\partial}{\partial z}(r\varepsilon w) = \frac{\partial}{\partial r} \left\{ r v_\theta \frac{\partial \varepsilon}{\partial r} \right\} + \frac{\partial}{\partial z} \left\{ r v_\theta \frac{\partial \varepsilon}{\partial z} \right\} + r \frac{\varepsilon}{k} \left(C_1 S - C_2 \varepsilon - C_3 g\beta \frac{v_\theta}{\sigma_\theta} \frac{\partial \theta}{\partial z} \right)$$

$$(6) \frac{\partial}{\partial t}(r\theta) + \frac{\partial}{\partial r}(r\theta u) + \frac{\partial}{\partial z}(r\theta w) = \frac{\partial}{\partial r} \left\{ r v_\theta \frac{\partial \theta}{\partial r} \right\} + \frac{\partial}{\partial z} \left\{ r v_\theta \frac{\partial \theta}{\partial z} \right\}$$

$$(7) v_i = C_D \frac{k^2}{\varepsilon}, \quad S = v_i \left\{ 2 \left(\frac{\partial u}{\partial r} \right)^2 + 2 \left(\frac{\partial w}{\partial z} \right)^2 + 2 \left(\frac{u}{r} \right)^2 + \left(\frac{\partial w}{\partial r} + \frac{\partial u}{\partial z} \right)^2 \right\}$$

$$v_\varepsilon = v + v_i, \quad v_k = v + \frac{v_i}{\sigma_k}, \quad v_\varepsilon = v + \frac{v_i}{\sigma_\varepsilon}, \quad v_\theta = a + \frac{v_i}{\sigma_\theta}$$

$$C_D = 0.09, \quad \sigma_k = 1.0, \quad \sigma_\varepsilon = 1.3, \quad \sigma_\theta = 1.0$$

$$C_1 = 1.44, \quad C_2 = 1.92, \quad C_3 = 0 \left(\frac{\partial \theta}{\partial z} > 0 \right) \text{ or } C_1 \left(\frac{\partial \theta}{\partial z} < 0 \right)$$

$$(8) C = \frac{a_p}{h} \times c\rho^* \times 3600 \quad (9) \frac{2\pi}{K} = \frac{1}{h_m r_{in}} + \frac{1}{\lambda_p} \ln \frac{r_{out}}{r_{in}}$$

$$(10) a_p = \frac{K \cdot r^*}{c\rho^* \times 3600} \quad r^* = \frac{h}{r_{out}}, \quad c\rho^* = 5.17 \text{ [MJ/m}^3\text{K]}$$

$$(11) Nu \equiv \frac{h_m 2r_{in}}{\lambda} = 1.86 \left(Re_d Pr \frac{2r_{in}}{l} \right)^{1/3} \quad \left(Re_d Pr \frac{2r_{in}}{l} > 12 \right)$$

$$l = 1.26 \text{ [m] the length of a cycle of coil}$$

$$(12) v = e^y \text{ [m}^2\text{/s]}$$

$$y = -9.0053 \times 10^{-7} t_w^3 + 2.3105 \times 10^{-4} t_w^2 - 3.2336 \times 10^{-2} t_w + 0.5681$$

$$(13) Pr = e^P$$

$$P = -1.2478 \times 10^{-6} t_w^3 + 2.9211 \times 10^{-4} t_w^2 - 3.7606 \times 10^{-2} t_w + 2.591$$

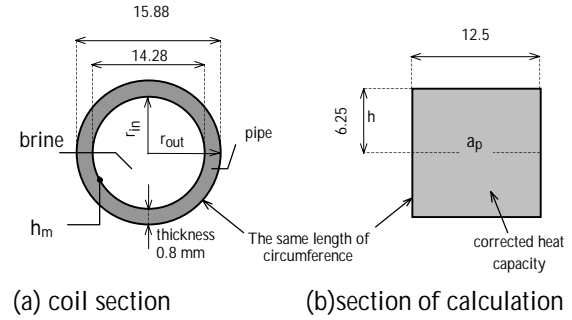
$$(14) \lambda = -6.3702 \times 10^{-6} t_w^2 + 1.7914 \times 10^{-3} t_w + 0.56962 \text{ [W/(mK)]}$$

Calculation of heat transfer from heat exchanger

(a) Setting of temperature diffusion coefficient within heat exchanger pipe

Temperature of brine within heat exchanger pipe can be solved by assuming that $v_\theta = ap$ and $u = w = 0$ using temperature diffusion coefficient ap in temperature transfer equation of the equation (6).

The value of ap is determined as given below by the modeling shown in Figure 4.



(a) coil section (b) section of calculation

Figure 4. Modeling of heat exchange pipe

Because cross-section of heat exchanger pipe was approximated by a lattice, brine and pipe material were combined for the calculation. It was assumed that heat conductance from brine in cylindrical pipe to pipe surface was C . Then, the equation (8) was obtained using average heat capacity of brine and pipe material, i.e. $c\rho^*$ and ap . Because the value of C can be obtained by dividing K in the equation (9) by surface area $2\pi r_{out}$, the value of ap can be obtained from the equation (10) by eliminating C .

Convective heat transfer coefficient (h_m) in heat exchanger pipe in the equation (9) is an important parameter to govern the heat transfer from heat exchanger pipe to inner space of heat storage tank. To simplify the calculation in the present study, Nusselt number was obtained from experimental equation of intra-pipe laminar flow heat transfer of the equation (11), and the value of h_m was calculated. Because physical property of water extensively varies according to temperature change, approximate expressions of the equations (12) - (14) were used for kinematic coefficient of viscosity (ν), Prandtl number (Pr) and thermal conductivity (λ).

(b) Approximation of brine heat transfer quantity by stationary calculation method

Brine is moved from inlet to outlet of heat exchanger in association with heat transfer, and temperature of brine in 12 pipes is gradually decreased. Normally, these temperature values can be obtained from the temperature transfer equation similar to the equation (6), but heat transfer may be overestimated very often due to false diffusion. In the present study, the stationary calculation method by Mizuno et al. was modified and used, and heat transfer quantity was treated in accordance with the following procedure as shown in Figure 5.

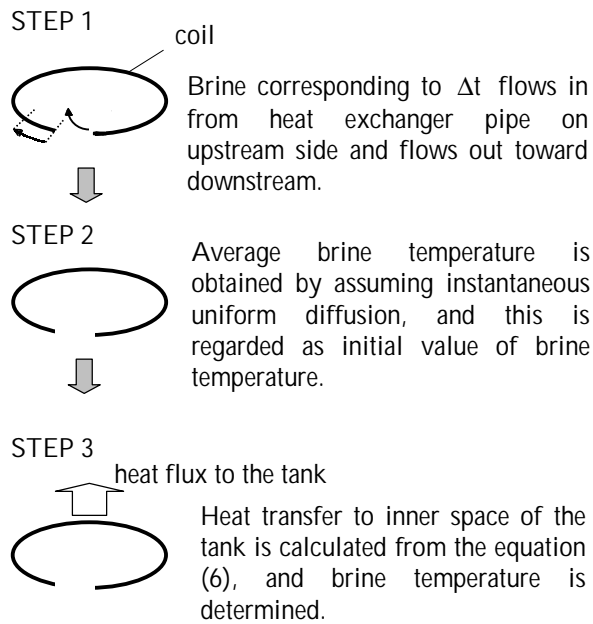


Figure 5. Heat flux from brine

Setting condition

Initial condition at the initiation of heat collecting is shown in Table 2. Initial values of k and ε were given in such manner that the initial value of v_t will be small enough with respect to v . Time differential interval (Δt) was set to 0.001 sec. to ensure the stability of calculation. During heat collecting, the value of Δt was adequately increased later to reduce the time of calculation.*1) During hot water supply, the value was set to a constant value of $dt = 0.001$ sec. from the initiation to the completion of hot water supply.

Table 2. Setting condition

heat storage when $t=0$	When supply hot water
water temp. 18.2 degree C	water flow rate: 15 litter/min.
inlet brine temperature from measurement data	$w=0.503$ m/s
$k_0=0.1235 \times 10^{-10}$ m ² /s ²	$k_{in}=0.1297 \times 10^{-2}$ m ² /s ²
$\varepsilon_0 = 0.2893 \times 10^{-11}$ m ² /s ³	$\varepsilon_{in} = 0.3382 \times 10^{-2}$ m ² /s ³
$\Delta t = 0.001$ second	$\Delta t = 0.001$ second

Because flow rate of brine was not determined, it was estimated from measurement data during the period of November 7 - 13. Difference between intra-tank temperature at the initiation of heat collecting operation and intra-tank temperature during hot water supply on each day was calculated. This value was multiplied by heat capacity of 1.265 MJ/K, and this was divided by the sum of the difference between

heat exchanger inlet temperature and outlet temperature of brine, and the flow rate was obtained.*2) From the average flow rate during 7 days under calculation, brine flow rate was determined as 7.2 liters/min.

CALCULATION RESULTS

The changes over time of the values such as brine outlet temperature and brine inlet temperature at the completion of heat collecting operation and during hot water supply, intra-tank average temperature, hot water feeding temperature, water feeding temperature, etc. are summarized in Figures 6 and 7. Figure 8 shows temperature distribution.

Changes over time of temperature values

In heat collecting operation, the measured values are adopted for brine inlet temperature. Brine outlet temperature suddenly decreased several times as shown in Figure 6, and this was because brine pump was controlled and was turned off. When brine temperature is unstable, e.g. at the initiation of heat collecting operation or frequent on/off control of brine pump, difference between the calculated values and the measured values is increased. In temperature increase of brine, both the calculated value and the measured value show similar tendency. The difference is about 1 deg. C at maximum, and the calculated value agrees with the experimental value. Daily total of heat collection quantity in the calculation is 48.0 MJ. When calculated from heat capacity of heat storage tank, temperature increase is obtained as about 38.2 deg. C. The temperature was turned from initial temperature of 18.2 deg. C to 56.4 deg. C at the termination of heat collecting operation, and this agreed well with the result of the calculation.

In Figure 7, the calculated result was consistent with the measured result in general tendency, but the decrease of hot water temperature was slightly delayed in the calculated result. This may be primarily attributed to the fact that axial symmetry was assumed in the present study. There are metal fittings and hardware to support hot water pipe and water supply pipe, and heat storage tank is not designed perfectly in axial symmetry in reality. In this respect, it appears that mixing of hot water and cold water in the tank is underestimated.

In the measurement schedule as used for comparison in this study, there was no case where heat collecting and hot water supply were performed at the same time, but, by the calculation method as used in the present study based on the comparison and the evaluation as described above, it appears that the numerical prediction can be achieved with sufficient accuracy.

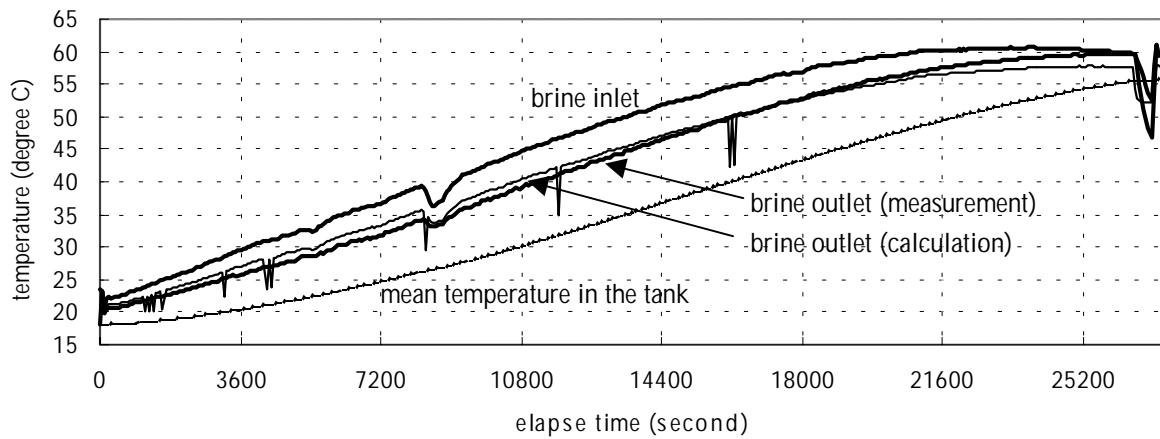


Figure 6. Calculation results in time change when heat storage

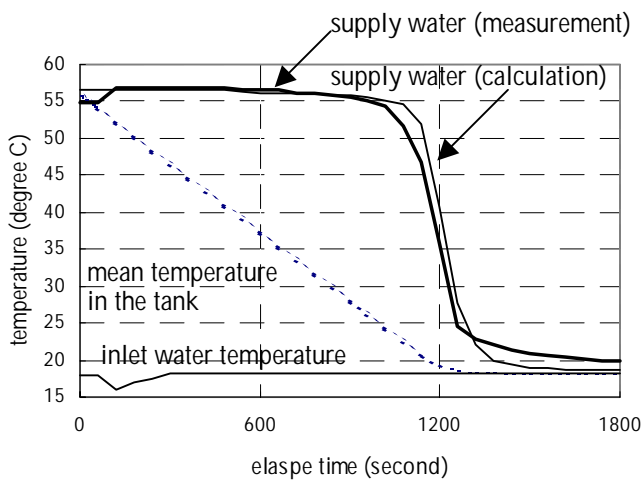
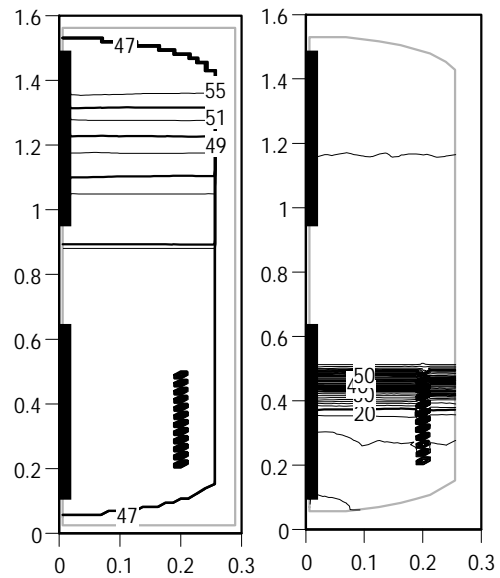


Figure 7. Calculation results when hot water supply



(a) heat storage after 6 hrs. (b) hot water supply after 5 min.

Figure 8. Calculated temperature distribution

Temperature distribution

In temperature distribution within the tank during heat collecting operation, a temperature stratified layer with gentle gradient is formed as shown in Figure 8(a). This is because natural convection occurs due to heat transfer from heat exchanger in the lower portion of the heat storage tank. This leads to the formation of relatively big vortex, and thorough mixing occurs within the tank.

During hot water supply, supplied water is spread along ellipsoid in the lower portion of the tank and a number of small vortexes are formed. In a portion where supply water and hot water are mixed together, a temperature stratified layer of about 150 mm in

height is generated as shown in Figure 8(b). As time elapses, this temperature stratified layer is moved upward, while keeping the stratified layer unchanged.

CONCLUSIONS

(i) Although there are limitations such as the setting of axial symmetry, the assumption of turbulent flow model, convection thermal conductivity within heat exchanger pipe, etc., we successfully established a calculation method to obtain flow behavior and temperature distribution in heat storage tank under unsteady condition using CFD.

(ii) Through comparison with the measured values, well-grounded and persuasive calculation results showing good agreement with the measured values

were obtained in both heat collecting and hot water supply. It appears that heat collection capacity from heat exchanger, transition of temperature distribution during hot water supply, etc. can be calculated with high accuracy for practical application. Even when heat collecting and hot water supply are performed at the same time, these values can be predicted by the calculation method established in the present study.

(iii) These calculation results cannot be easily obtained by actual measurement. It should be the subject theme in the future study to reflect these calculation results in block model and to develop a method of numerical prediction, which gives accurate calculation results within shorter time.

ACKNOWLEDGMENT

The author extends sincere gratitude to Mr. Shunji Asai of YAZAKI CORPORATION and other persons for their kind cooperation and advice with regard to general features and measurement data of the heat storage tank.

REFERENCES

ASHRAE Handbook Fundamentals 1997.

Mizuno et al., Thermal Analysis and Economical Thickness of Thermal Insulation Material of Intermittently Used Hot Water Supply Pipeline (in Japanese), Transactions of SHASEJ, No.52, pp.29-38, 1993.

NOTES

*1 All calculations in the present study have been executed using personal computer incorporated with DEC Alpha 21164A/600 MHz. The time of calculation was 90 hours for heat collecting, and 9 hours for hot water supply.

*2 As brine, 33% aqueous solution of propylene glycol should be used. In the present study, water was used instead for simplification of the procedure.